JOURNAL OF MATERIALS SCIENCE **38** (2003) 4849–4856

Mechano-electrochemical effect between erosion and corrosion

JIANHUI XIE*,‡, A. T. ALPAS, D. O. NORTHWOOD
Department of Mechanical, Automotive and Materials Engineering, University of Windsor, 401 Sunset Avenue, Windsor, ON, Canada N9B 3P4
E-mail: jeffrey.xie@nrc-cnrc.gc.ca

The characteristics and mechanisms of the mechano-electrochemical effect were investigated both theoretically and experimentally for two steels (AISI 1020 and 52100) in various heat-treated conditions subjected to sequential erosion and corrosion. A mathematical equation is developed to describe the mechano-electrochemical effect in which the corrosion rate is exponentially related to the change of corrosion potential and increased stored strain energy.

The agreement between calculated and measured corrosion rate is good for the annealed AISI 1020 steel and both the annealed and the tempered AISI 52100 steels, in which the microstrain and stored strain energy originate only from erosion.

1. Introduction

The mechano-electrochemical effect is defined as the influence of plastic deformation on electrochemical characteristics and parameters of anodic polarization [1–10]. The mechano-electrochemical effect would be present in an environment comprised of mechanical action (causing deformation) and a corrosive agent. In the mechano-electrochemical effect, the mechanical effect, which causes deformation, and thus increases the strain energy, significantly increases the corrosion rate. A significant mechano-electrochemical effect manifests itself in the values of corrosion rate, corrosion potential, and polarization resistance.

The mechano-electrochemical effect is usually expressed in a literal description, or as a graph where an electrochemical parameter is plotted as a function of the load or strain [11–15]. To quantitatively describe the mechano-electrochemical effect, a mathematical equation must be developed to describe the relationship between the electrochemical parameters and the load or strain. Since the corrosion rate (current density) generally reflects other parameters, such as potential, polarization resistance, etc., it can be used as a generalized parameter to characterize the mechano-electrochemical effect.

In this investigation, a theoretical analysis was made of the mechano-electrochemical effect, and a quantitative correlation was established between the corrosion rate and the corrosion potential, strain energy and polarization behavior. The increased corrosion rate due to plastic deformation can be calculated from this kinetic equation, and the calculated corrosion rate is found to agree with the experimentally measured corrosion rates for two steels subjected to sequential erosion and corrosion.

2. Theoretical analysis of mechano-electrochemical effect

2.1. Mechano-electrochemical activity of a deformed electrode

The electrochemical potential, μ_e, of an electrochemical reaction $R \Leftrightarrow O + ne^-$ (where R is the reductive reactant and, O is the oxidative reactant) can be expressed as follows [16–18]:

$$\mu_e = \mu + nF\varepsilon = \mu_0 + RT\ln a + nF\varepsilon \qquad (1)$$

where μ is the chemical potential, n is the valence of the reactant, F is Faraday constant, ε is the potential of the reaction system, μ_0 is the standard chemical potential, a is the activity of the reactant, R is the gas constant and T is the temperature in degrees Kelvin.

If a metallic electrode is subjected to deformation, and a residual stress, ΔP, is present in the deformed electrode, the chemical potential, μ_s, of the deformed electrode (stressed electrode) can be expressed as [17]:

$$\mu_s = \mu_{\Delta P=0} + \Delta P \cdot V = \mu_0 + RT\ln a + \Delta P \cdot V \qquad (2)$$

where V is the volume of the deformed metal.

If the metal electrode is subjected to a combination of mechanical and electrochemical effects, the mechano-electrochemical potential, μ_{se}, can be obtained from

Current address: Institute for Chemical Process & Environmental Technology, National Research Council Canada, 1200 Montreal Road, Ottawa, Ontario, Canada K1A 0R6.
‡Author to whom all correspondence should be addressed.

Equations 1 and 2 as follows [17]:

$$\mu_{se} = \mu_0 + RT \ln a + \Delta P \cdot V + nF\varepsilon \quad (3)$$

According to the definition of chemical potential [17]:

$$\mu = \mu_0 + RT \ln a \quad (4)$$

Thus, the mechano-electrochemical potential, μ_{se}, can be expressed as:

$$\begin{aligned}\mu_{se} &= \mu_0 + RT \ln a + \Delta P \cdot V + nF\varepsilon \\ &= \mu_0 + RT \ln a_{se}\end{aligned} \quad (5)$$

The mechano-electrochemical activity, a_{se}, can then be obtained from Equation 5:

$$a_{se} = ae^{(nF\varepsilon + \Delta P \cdot V)/RT} = ae^{(nF\varepsilon + A)/RT} \quad (6)$$

where $A = \Delta P \cdot V$ is the strain energy due to the deformation from the mechanical action.

For an electrochemical reaction that is subject to electrochemical polarization, when the potential shifts from ε_e (equilibrium potential) to ε with a change $\Delta\varepsilon = \varepsilon - \varepsilon_e$, the potential change of the deformed electrode is $\alpha\Delta\varepsilon$, and the potential change of the ions in the solution is $\beta \cdot \Delta\varepsilon$ (where α, β are the exchange coefficients, and $\alpha + \beta = 1$). Thus the mechano-electrochemical activity of the deformed metal electrode due to an overpotenial of $\Delta\varepsilon$ can be expressed as:

$$a_{se} = ae^{(nF(\alpha \cdot \Delta\varepsilon) + A)/RT} = ae^{(\alpha nF\Delta\varepsilon + A)/RT} \quad (7)$$

2.2. Reaction kinetics of a deformed electrode with a single reaction

The activation energies, W, of the anodic and cathodic reactions for an undeformed electrode with an overpotential of $\Delta\varepsilon$ are as follows [17]:

$$W_1 = W_1^0 - \beta nF\Delta\varepsilon \quad (8)$$

$$W_2 = W_2^0 + \alpha nF\Delta\varepsilon \quad (9)$$

where W_1^0 and W_2^0 are the individual activation energies for the oxidation reaction and reduction reaction at equilibrium conditions.

The relationship between the reaction rate, V, and the current density is [17]:

$$i = nFV \quad (10)$$

According to the Arrhenius relationship [17]:

$$V = ZCe^{-(W/RT)} \quad (11)$$

where V is the reaction rate, Z is a constant, and C is the concentration of the reactant.

The current density can be expressed as follows:

$$i = nFV = nFZCe^{-(W/RT)} = nFKC \quad (12)$$

where $K = Ze^{-(W/RT)}$.

Thus the exchange current density, i^0, at equilibrium potential is given by:

$$\begin{aligned}i^0 &= nF\vec{Z}C_R e^{-W_1^0/RT} = nF\overleftarrow{Z}C_O e^{-W_2^0/RT} \\ &= nF\vec{K}_0 C_R = nF\overleftarrow{K}_0 C_O\end{aligned} \quad (13)$$

The corresponding rates of the anodic and cathodic reactions at polarization with an overpotential of $\Delta\varepsilon$ can be written as:

$$\begin{aligned}\left|\vec{i}\right| &= nF\vec{Z}\,C_R e^{-(W_1^0 - \beta nF\Delta\varepsilon)/RT} \\ &= nF\vec{Z}\,C_R e^{-W_1^0/RT} e^{\beta nF\Delta\varepsilon/RT} \\ &= nF\vec{K}_0\,C_R e^{\beta nF\Delta\varepsilon/RT}\end{aligned} \quad (14)$$

$$\begin{aligned}\left|\overleftarrow{i}\right| &= nF\overleftarrow{Z}C_O e^{-(W_2^0 + \alpha nF\Delta\varepsilon)/RT} \\ &= nF\overleftarrow{Z}C_O e^{-W_2^0/RT} e^{-(\alpha nF\Delta\varepsilon/RT)} \\ &= nF\overleftarrow{K}_0 C_O e^{-(\alpha nF\Delta\varepsilon/RT)}\end{aligned} \quad (15)$$

Equations 14 and 15 are the anodic and cathodic reaction rates of an undeformed metal electrode. When they are equal to each other at the equilibrium potential, $|\vec{i}|$ and $|\overleftarrow{i}|$ become the exchange current density i^o. When the metal electrode is subjected to deformation, the activity of the metallic ion in the metal electrode is changed and is as given in Equation 7, while the activity of the ion in solution does not change. If it is valid to replace concentration with activity in a metallic electrode, then the reaction rate of the deformed metal electrode can be obtained by substituting Equation 7 into Equation 14. Then Equations 14 and 15 become as follows:

$$\begin{aligned}\left|\vec{i}\right|^s &= nF\vec{K}_0\,a_{seR} e^{\beta nF\Delta\varepsilon/RT} \\ &= nF\vec{K}_0\,a_R e^{(\alpha nF\Delta\varepsilon + A)/RT} e^{\beta nF\Delta\varepsilon/RT}\end{aligned} \quad (16)$$

$$\left|\overleftarrow{i}\right|^s = nF\overleftarrow{K}_0 C_O e^{-(\alpha nF\Delta\varepsilon/RT)} \quad (17)$$

Substituting the exchange current density Equation 13 into Equations 16 and 17; one obtains:

$$\begin{aligned}\left|\vec{i}\right|^s &= i^0 e^{(\alpha nF\Delta\varepsilon + A)/RT} e^{\beta nF\Delta\varepsilon/RT} \\ &= i^0 e^{(nF\Delta\varepsilon + A)/RT}\end{aligned} \quad (18)$$

$$\left|\overleftarrow{i}\right|^s = i^0 e^{-(\alpha nF\Delta\varepsilon/RT)} \quad (19)$$

Thus for the deformed metal electrode subjected to anodic polarization with an overpotential of $\Delta\varepsilon$, the net polarization current, i_a^s (anodic reaction rate) can be

expressed as follows:

$$i_a^s = \left|\vec{i}\right|^s - \left|\overleftarrow{i}\right|^s = i^0\left(e^{nF\Delta\varepsilon/RT}e^{A/RT} - e^{-(\alpha nF\Delta\varepsilon/RT)}\right)$$
$$= i^0\left(e^{(\beta nF/RT)\eta_a^s}e^{A/RT} - e^{-(\alpha nF/RT)\eta_a}\right) \quad (20)$$

where $\eta_a = \varepsilon - \varepsilon_e$ is the overpotential ($\Delta\varepsilon$) of undeformed electrode, and $\eta_a^s = \Delta\varepsilon/\beta$ is the overpotential of deformed metal electrode. Since $\beta < 1$, then $\eta_a^s > \eta_a$, and $e^{A/RT}$ is also greater than unity, thus the reaction rate, i_a^s, of a deformed electrode is higher than for an undeformed electrode, i_a, which is given by:

$$i_a = \left|\vec{i}\right| - \left|\overleftarrow{i}\right| = i^0\left(e^{(\beta nF/RT)\eta_a} - e^{-(\alpha nF/RT)\eta_a}\right) \quad (21)$$

Since $\eta_a^s > \eta_a$, for the same polarization potential (ε), based on the definition of $\eta_a = \varepsilon - \varepsilon_e$, the equilibrium potential (ε_e) of the deformed electrode will be lower than that of the undeformed electrode. The fact that i_a^s is larger than i_a demonstrates that the reaction rate (corrosion rate) of a deformed electrode is greater than that of an undeformed electrode. This is the mechano-electrochemical effect, leading to a synergistic increase in material loss due to mechanical and electrochemical actions.

2.3. Reaction kinetics of a deformed electrode in a corrosive environment

The corrosion reaction of eroded steel specimens in a corrosive environment is a combination of multi-electrode reactions ($M \Leftrightarrow M^{n+} + ne$ and $R \Leftrightarrow O + ne$). If all anodic and cathodic reactions are controlled by activation polarization, and their reaction kinetics follow the Tafel equation, the corresponding anodic reaction of $M \Leftrightarrow M^{n+} + ne$, and cathodic reaction of $R \Leftrightarrow O + ne$ could be neglected, and thus the anodic and cathodic current of a deformed electrode in a corrosive environment can be described by the simplified relationships, based on Equations 20 and 21:

$$i_a^s = i_a^0 e^{(\beta nF/RT)\eta_a^s}e^{A/RT} \quad (22)$$

$$i_c = i_c^0 e^{-(\alpha nF/RT)\eta_c} \quad (23)$$

Thus the net reaction current (the current density in the circuit), I_A^s, for corrosion reactions in a deformed electrode can be expressed as:

$$I_A^s = i_a^s - i_c = i_a^o e^{(\beta nF/RT)\eta_a^s}e^{A/RT} - i_c^0 e^{-(\alpha nF/RT)\eta_c}$$
$$= i_a^0 e^{(E-E_{e,a}^s)/b_a}e^{A/RT} - i_c^0 e^{(E_{e,c}-E)/b_c} \quad (24)$$

where $E - E_{e,a}^s = \eta_a^s$ is the anodic overpotential of the corrosion reaction, $E_{e,c} - E = \eta_c$ is the cathodic overpotential of the corrosion reaction, $b_a = RT/\beta nF$ is the anodic Tafel slope of the potentiodynamic polarization curve, and $b_c = RT/\alpha nF$ is the cathodic Tafel slope of the potentiodynamic polarization curve.

To obtain the relationship between the anodic reaction rate (corrosion rate) of the deformed electrode and the undeformed electrode in a corrosive environment, Equation 24 is modified to:

$$I_A^s = i_a^0 e^{\{(E-E_k)+(E_k-E_{e,a})+(E_{e,a}-E_{e,a}^s)\}/b_a}e^{A/RT}$$
$$- i_c^0 e^{\{(E_{e,c}-E_k)+(E_k-E)\}/b_c}$$
$$= i_a^0 e^{(E_k-E_{e,a})/b_a}e^{(E-E_k+\Delta E_{e,a}^s)/b_a}e^{(A/RT)}$$
$$- i_c^0 e^{(E_{e,c}-E_k)/b_c}e^{(E_k-E)/b_c} \quad (25)$$

where E_k is the corrosion potential of an un-deformed specimen when the net polarization current density is zero, $\Delta E_{e,a}^s = E_{e,a} - E_{e,a}^s$. Because the corrosion current at a corrosion potential of E_k can be expressed as [17]:

$$i_k = i_a^0 e^{(E_k-E_{e,a})/b_a} = i_c^0 e^{(E_{e,c}-E_k)/b_c} \quad (26)$$

Then, by substituting Equation 26 into Equation 25, we obtain:

$$I_A^s = i_k e^{(E-E_k+\Delta E_{e,a}^s)/b_a}e^{A/RT} - i_k e^{(E_k-E)/b_c}$$
$$= i_k\left(e^{(E-E_k^s)/b_a}e^{A/RT} - e^{(E_k-E)/b_c}\right) \quad (27)$$

where $E_k^s = E_k - \Delta E_{e,a}^s$ is defined as the corrosion potential of the deformed electrode in a corrosion environment at a net polarization current of zero. Thus, it is concluded that the corrosion potential of the reaction for the deformed specimens is lower (with a magnitude of $\Delta E_{e,a}^s$) than that for undeformed specimens. Comparing the net polarization current Equation 27 for the deformed electrode in a corrosion environment with the net polarization current Equation 28 for the undeformed electrode system, it is concluded that deformation increases the net polarization current.

$$I_A = i_k\left(e^{(E-E_k)/b_a} - e^{(E_k-E)/b_c}\right) \quad (28)$$

2.4. Mathematical expression of corrosion rate for a deformed electrode in a corrosion environment

The polarization kinetics Equation 27 of a reaction for a deformed electrode in a corrosion system can be further modified as follows:

$$I_A^s = i_k e^{(E-E_k)/b_a}e^{\Delta E_k^s/b_a}e^{A/RT} - i_k e^{(E_k-E)b_c} \quad (29)$$

where $\Delta E_k^s = E_k - E_k^s$ is defined as the change in the corrosion potential of a deformed electrode from the potential of an undeformed electrode.

In an electrochemical reaction in a corrosion system, if it is assumed that the anodic and cathodic reactions in a corrosion process are controlled by activation polarization, and that the reaction kinetics follow a Tafel relationship, then the rates of the anodic and cathodic reactions are given by:

$$i_A = i_k e^{(E-E_k)/b_a} \quad (30)$$

$$i_C = i_k e^{(E_k-E)/b_c} \quad (31)$$

Substituting Equations 30 and 31 into Equation 29 gives:

$$I_{\mathrm{A}}^{\mathrm{s}} = i_{\mathrm{A}}^{\mathrm{s}} - i_{\mathrm{C}}^{\mathrm{s}} = i_{\mathrm{A}}^{\mathrm{s}} - i_{\mathrm{C}} = i_{\mathrm{A}} e^{\Delta E_{\mathrm{k}}^{\mathrm{s}}/b_{\mathrm{a}}} e^{A/RT} - i_{\mathrm{C}} \quad (32)$$

This equation is defined as the net current for corrosion reactions of the deformed electrode in a corrosion system. Thus the anodic reaction rate (corrosion rate) can be expressed as:

$$i_{\mathrm{A}}^{\mathrm{s}} = i_{\mathrm{A}} e^{\Delta E_{\mathrm{k}}^{\mathrm{s}}/b_{\mathrm{a}}} e^{A/RT} \quad (33)$$

Equation 33 is the mathematical expression of the mechano-electrochemical effect. The product of two exponential parts in this equation is greater than unity, thus $i_{\mathrm{A}}^{\mathrm{s}} > i_{\mathrm{A}}$. It can be concluded that the corrosion rate of the deformed electrode is larger than that of the undeformed electrode and that the increased anodic corrosion rate depends on two factors, namely (i) the stored strain energy (A) and (ii) the decreased corrosion potential ($\Delta E_{\mathrm{k}}^{\mathrm{s}}$). This is the mechanism of the synergistic effect between erosion and corrosion—a mechano-electrochemical effect whereby the erosion action increases the corrosion rate.

3. Experimental verification of the mechano-electrochemical effect

AISI 1020 and 52100 were chosen as the testing materials. The as-received AISI 52100 steel was further heat-treated by annealing (750°C, furnace cooling), quenching (900°C, quenched in water) or tempering (650°C). Similarly, the as-received AISI 1020 steel was heat-treated by annealing (870°C, furnace cooling) or quenching (900°C, quenched in water).

Dry erosion testing was carried out in a customized erosion tester [19]. The erodent, which is SiC particles with size of 120 grit, is carried along a steel pipe (20 mm in outer diameter and 2 mm in wall thickness and 1500 mm in length) by pressurized air to impact on the steel specimen at a velocity of 38 m/s. The amount of erodent was 0 g (i.e. uneroded), 10, 50 and 100 g. The erosion angle was set at 45°.

Electrochemical measurements were conducted in a solution of 2 g/L NaCl and 2 g/L Na_2SO_4 (adjusted to neutral pH value) using a Solartron 1285 Potentiostat/Galvanostat and CorrView software, and a tri-electrode cell. The eroded/uneroded specimens were used as the working electrodes (WE). A saturated calomel electrode (SCE) was used as the reference electrode (RE) and a graphite plate was used as the counter electrode (CE).

TABLE IA Electrochemical parameters and strain energy of AISI 52100 steel obtained from experimental measurements

Heat treatment	Electrochemical parameters & strain energy	Value of parameters			
		No erosion	10 g erodent	50 g erodent	100 g erodent
As-received	Polarization resistance ($\Omega \cdot cm^2$)	1600	1547	1367	1228
	Tafel slopes				
	b_a (V)	0.0561	0.0629	0.0705	0.0734
	b_c (V)	−0.0348	−0.2165	−0.1707	−0.1371
	B	0.0093	0.0212	0.0217	0.0208
	Corrosion potential (V, SCE)	−0.419	−0.689	−0.692	−0.697
	$\Delta E_{\mathrm{k}}^{\mathrm{s}}$ (V)	0	0.270	0.273	0.278
	Strain energy (J/mol)	90	1968	1993	2750
	Corrosion rate ($\times 10^{-5}$ A/cm^2)	0.5829	1.3680	1.5848	1.6904
Annealed	Polarization resistance ($\Omega \cdot cm^2$)	1287	1145	829	801
	Tafel slopes				
	b_a (V)	0.0486	0.0606	0.0558	0.0681
	b_c (V)	−0.1828	−0.1338	−0.1543	−0.2801
	B	0.0167	0.0181	0.0178	0.0238
	Corrosion potential (V, SCE)	−0.662	−0.669	−0.671	−0.719
	$\Delta E_{\mathrm{k}}^{\mathrm{s}}$ (V)	0	0.007	0.009	0.057
	Strain energy (J/mol)	0	1004	2266	2648
	Corrosion rate ($\times 10^{-5}$ A/cm^2)	1.2953	1.5817	2.1465	2.9697
Quenched	Polarization resistance ($\Omega \cdot cm^2$)	1711	1187	1102	849
	Tafel slopes				
	b_a (V)	0.0539	0.0517	0.0677	0.0750
	b_c (V)	−0.1256	−0.1969	−0.2767	−0.2043
	B	0.0164	0.0178	0.0236	0.0238
	Corrosion potential (V, SCE)	−0.403	−0.62	−0.675	−0.697
	$\Delta E_{\mathrm{k}}^{\mathrm{s}}$ (V)	0	0.217	0.272	0.294
	Strain energy (J/mol)	2249	3046	9491	13640
	Corrosion rate ($\times 10^{-5}$ A/cm^2)	0.9571	1.4979	2.1432	2.8058
Tempered	Polarization resistance ($\Omega \cdot cm^2$)	1592	1548	1372	1237
	Tafel slopes				
	b_a (V)	0.0510	0.0683	0.0694	0.0637
	b_c (V)	−0.1730	−0.1987	−0.3240	−0.7761
	B	0.0171	0.0221	0.0248	0.0256
	Corrosion potential (V, SCE)	−0.563	−0.639	−0.672	−0.683
	$\Delta E_{\mathrm{k}}^{\mathrm{s}}$ (V)	0	0.076	0.109	0.12
	Strain energy (J/mol)	6	1070	1157	1725
	Corrosion rate ($\times 10^{-5}$ A/cm^2)	1.0743	1.4258	1.8089	2.0664

The electrochemical measurements were made for the eroded specimens immediately after the erosion test (The eroded surface was first blown clean by pressurized air). The specimens were sealed using waterproof adhesive tape to expose only a small eroded area (about 0.5 to 1.0 cm^2, used to calculate the current density by dividing the current by the area) of the specimen to the solution and to protect the connecting clips.

The electrochemical experiments that were performed [20] included the measurement of: (i) open circuit potentials; (ii) polarization resistance from linear polarization curves; (iii) Tafel slopes from potentiodynamic polarization curves on samples, which were eroded with different amounts (10, 50 and 100 g) of SiC particles. These results were compared with those from uneroded samples. The corrosion rates were calculated using the following Equation 21:

$$i_k = \frac{B}{R_p} \tag{34}$$

where $B = (b_a \cdot b_c)/(2.303(b_a + b_c))$, b_a and b_c are the Tafel slopes of anodic and cathodic polarization curves, and R_p is the polarization resistance. All these parameters were obtained from the electrochemical measurements [20].

The microstrain was measured using the broadening of the X-ray Diffraction (XRD) peaks and can be obtained from a slope of the plot of $B_r \cdot \cos\theta$ vs $\sin\theta$ using Equation 35 [22]:

$$B_r \cos\theta = \eta \sin\theta + \frac{k\lambda}{L} \tag{35}$$

where $B_r = \sqrt{B_o^2 - B_i^2}$, k is a constant, λ is the wavelength of incident X-rays, L is the average crystallite size, η is the microstrain, B_o is the width of the peak at half the maximum intensity of the observed X-ray peak and B_i is the width at the half maximum intensity of the X-ray peak of a fully annealed sample.

The corresponding stored strain energy, A, can be calculated as follows [23]:

$$A = \frac{15E}{2(3 - 4\upsilon + 8\upsilon^2)} \cdot \left(\frac{\Delta d}{d}\right)^2 \tag{36}$$

where E is Young's modulus, $\frac{\Delta d}{d} = 2\eta$ and υ is Poisson's ratio.

Tables IA and B give a summary of the electrochemical parameters and strain energy obtained from the experimental measurements for both the AISI 51200 and 1020 steels [21].

Fig. 1a and b illustrate the relationship between the experimentally measured corrosion rates and the potential change for both the AISI 52100 and 1020 steels. There is an exponential relationship between corrosion rate and potential change with a good R value, which is consistent with Equation 33.

Fig. 2a and b illustrate the relationship between the experimentally measured corrosion rates and the strain

TABLE IB Electrochemical parameters and strain energy of AISI 1020 steel obtained from experimental measurements

Heat treatment	Electrochemical parameters & strain energy	Value of parameters			
		No erosion	10 g erodent	50 g erodent	100 g erodent
As-received	Polarization resistance ($\Omega \cdot cm^2$)	1552	1339	1308	1269
	Tafel slopes				
	b_a (V)	0.0613	0.0589	0.0763	0.0770
	b_c (V)	−0.1862	−0.2883	−0.5393	−0.5882
	B	0.0200	0.0212	0.0290	0.0296
	Corrosion potentials (V, SCE)	−0.636	−0.692	−0.765	−0.776
	ΔE_k^s (V)	0	0.056	0.129	0.14
	Strain energy (J/mol)	52	684	794	1962
	Corrosion rate ($\times 10^{-5}$ A/cm^2)	1.2903	1.5860	2.2190	2.3297
Annealed	Polarization resistance ($\Omega \cdot cm^2$)	1145	1009	994	996
	Tafel slopes				
	b_a (V)	0.0293	0.0637	0.0636	0.1045
	b_c (V)	−0.2533	−0.1454	−0.1888	−0.1905
	B	0.0114	0.0192	0.0207	0.0299
	Corrosion potential (V, SCE)	−0.727	−0.738	−0.744	−0.784
	ΔE_k^s (V)	0	0.011	0.017	0.057
	Strain energy (J/mol)	0	916	1590	1798
	Corrosion rate ($\times 10^{-5}$ A/cm^2)	0.9959	1.9062	2.0782	2.9420
Quenched	Polarization resistance ($\Omega \cdot cm^2$)	1539	1070	805	775
	Tafel slopes				
	b_a (V)	0.0688	0.0692	0.0643	0.0682
	b_c (V)	−0.1325	−0.1303	−0.2248	−0.2192
	B	0.0197	0.0196	0.0217	0.0226
	Corrosion potential (V, SCE)	−0.570	−0.675	−0.672	−0.708
	ΔE_k^s (V)	0	0.105	0.102	0.138
	Strain energy (J/mol)	110	623	853	1305
	Corrosion rate ($\times 10^{-5}$ A/cm^2)	1.2777	1.8341	2.6969	2.9144

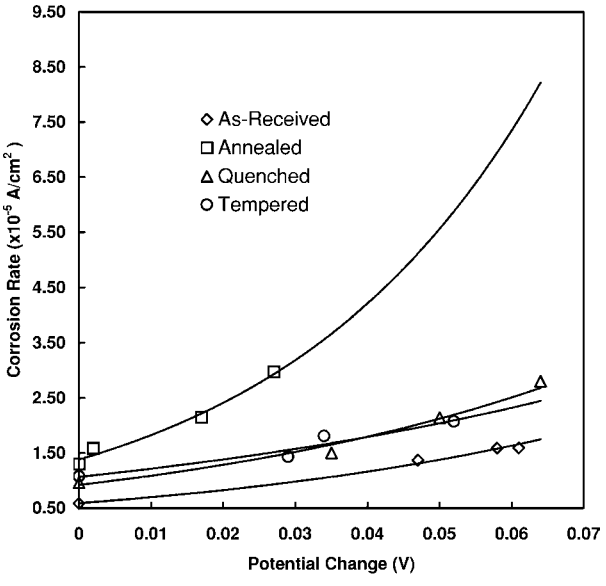

(a)

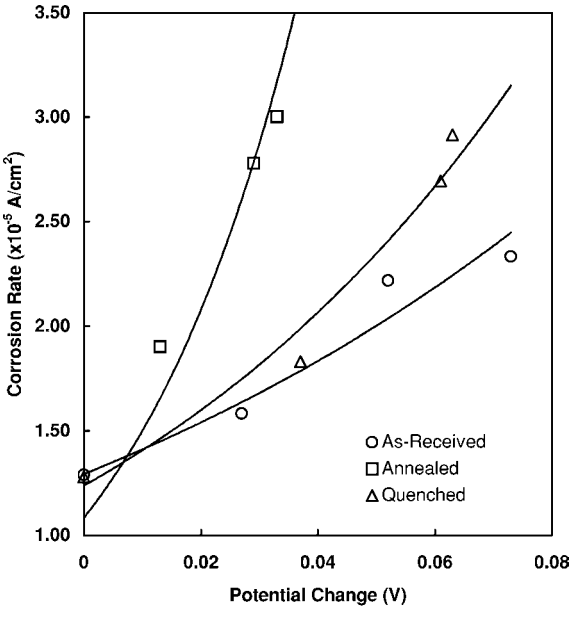

(b)

Figure 1 The relationship between corrosion rate and the potential change for (a) AISI 52100 steel (As-received: $i_{corr} = 0.5877e^{17.016(\Delta E)}$ with $R^2 = 0.994$; Annealed: $i_{corr} = 1.3805e^{27.864(\Delta E)}$ with $R^2 = 0.971$; Quenched: $i_{corr} = 0.9196e^{16.712(\Delta E)}$ with $R^2 = 0.9798$ and Tempered: $i_{corr} = 1.0667e^{12.942(\Delta E)}$ with $R^2 = 0.9403$) and (b) AISI 1020 steels (As-received: $i_{corr} = 1.2929e^{8.741(\Delta E)}$ with $R^2 = 0.9555$; Annealed: $i_{corr} = 1.0837e^{32.52(\Delta E)}$ with $R^2 = 0.9609$ and Quenched: $i_{corr} = 1.2375e^{12.805(\Delta E)}$ with $R^2 = 0.9761$).

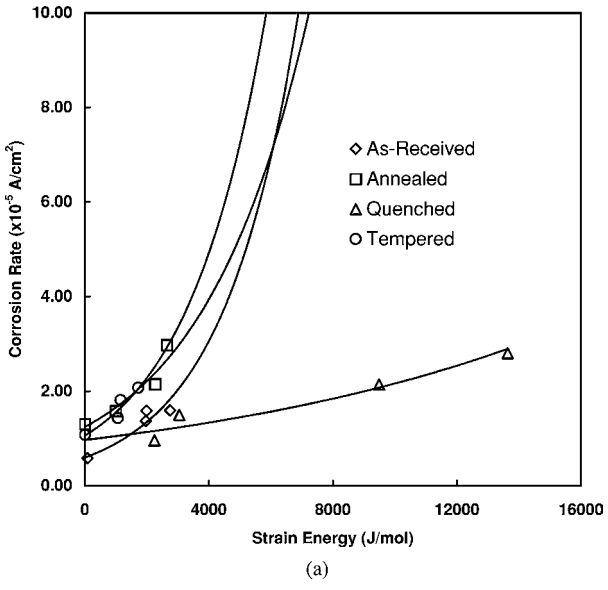

(a)

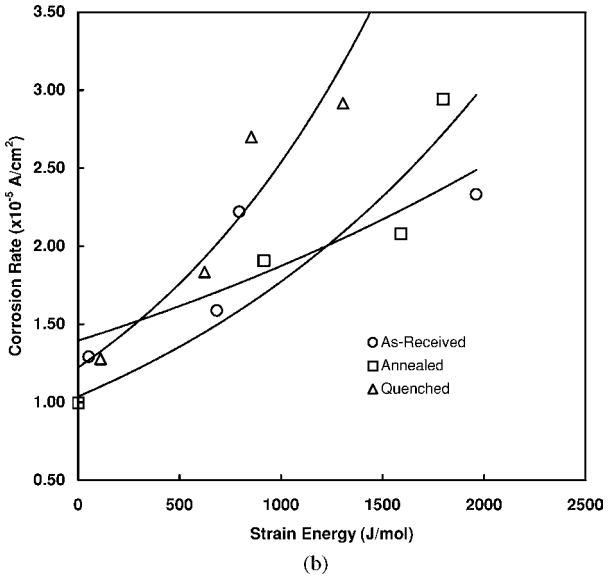

(b)

Figure 2 The relationship between corrosion rate and strain energy for (a) AISI 52100 steels (As-received: $i_{corr} = 0.5928e^{0.0004A}$ with $R^2 = 0.9255$; Annealed: $i_{corr} = 1.2406e^{0.0003A}$ with $R^2 = 0.9307$; Quenched: $i_{corr} = 0.968e^{8E-5A}$ with $R^2 = 0.8832$ and Tempered: $i_{corr} = 1.0583e^{0.0004A}$ with $R^2 = 0.9157$) and (b) AISI 1020 steels (As-received: $i_{corr} = 1.3937e^{0.0003A}$ with $R^2 = 0.693$; Annealed: $i_{corr} = 1.0363e^{0.0005A}$ with $R^2 = 0.9243$ and Quenched: $i_{corr} = 1.2221e^{0.0007A}$ with $R^2 = 0.9099$).

energy caused by erosion for AISI 52100 and 1020 steels, respectively. There is an exponential relation between the corrosion rate and the strain energy with a reasonably good R value except for the as-received AISI 1020 steel, where the exponential relationship has a R value of only 0.699, i.e., the results are consistent with Equation 33.

To test the theoretically developed mechano-electrochemical equations, the corrosion rates of eroded AISI 52100 and AISI 1020 steels were calculated using Equation 33 and the experimentally measured values of the decrease in corrosion potential (ΔE_k^s) and the stored strain energy (A). It is assumed that the corrosion reaction takes place at a temperature of 25°C.

The calculated corrosion rates for the AISI 52100 steel are given in Table IIA and compared with the experimentally measured corrosion rates. There are considerable differences between the measured and calculated corrosion rates, especially for the as-received and quenched AISI 52100 steel specimens. The agreement between the two rates is reasonable for both the annealed and the tempered samples.

The mechano-electrochemical Equation 33 was derived by taking into account only the plastic deformation caused by mechanical effect, which in this investigation was erosion by SiC particles. In both the annealed and the tempered specimens the microstrain

TABLE IIA Comparison of the calculated and experimental corrosion rates for eroded AISI 52100 steel

AISI 52100 steels	Corrosion rate i_a^s	Corrosion rate ($\times 10^{-5}$ A/cm^2) Amount of erodent (erosion angle 45°) No erosion	10 g	50 g	100 g
As-received	Experimental corrosion rate	0.58	1.37	1.58	1.69
	Calculated corrosion rate	0.62	94.36	62.62	78.08
Annealed	Experimental corrosion rate	1.30	1.59	2.15	2.97
	Calculated corrosion rate	1.30	2.18	3.80	8.71
Tempered	Experimental corrosion rate	1.07	1.33	1.71	1.99
	Calculated corrosion rate	1.08	5.03	8.24	14.18
Quenched	Experimental corrosion rate	0.96	1.50	2.14	2.81
	Calculated corrosion rate	2.37	217.65	2451.96	11967.31

(thus the increased stored strain energy) arises only from erosion and the calculated corrosion rates agree reasonably well with the experimentally measured corrosion rates. For both the quenched and the as-received specimens there are microstrains induced also from the heat treatment or residual cold-work, and the calculated corrosion rates deviate significantly from the experimentally measured corrosion rates, which reflect the total stored energy not just that induced by erosion.

If a graph of calculated corrosion rate vs. the experimental corrosion rate is plotted, a linear regression line can be plotted. The fit to a linear relationship is best for the annealed specimens with $R^2 = 0.97$, and the tempered specimens with $R^2 = 0.96$ (Fig. 3a). The annealed specimen has no residual stress after heat treatment, and the stored strain energy only arises from the impact of the SiC particles on the surface. The tempering treatment eliminates the large distortion due to quenching. For the as-received and quenched specimens, which have residual stresses due to cold work or distortion due to the quenching treatment, a deviation from a linear relationship is observed ($R^2 = 0.74$ for the as-received and 0.79 for the quenched samples).

A similar exercise was undertaken using the results for the AISI 1020 steel. The calculated corrosion rates of the AISI 1020 steel are given in Table IIB and compared with the experimentally measured corrosion rates. There are considerable differences between the experimentally measured and calculated corrosion rates, especially for the as-received and quenched AISI 1020 specimens. For the annealed specimens, the differences are small.

If a graph of the calculated corrosion rate vs. the experimentally measured corrosion rate is plotted, there is a linear relationship. The fit is especially good for the annealed specimens with $R^2 = 0.94$ (Fig. 3b). As for the AISI 52100 steel, annealing eliminates the residual microstrains, and the stored strain energy arises only from the erosion. For the as-received and quenched 1020 steel specimens, which have microstrains due to cold work or distortion from the quenching treatment, a deviation from a linear relationship is observed as for AISI 52100 steel ($R^2 = 0.86$ for the a-received and 0.81 for the quenched samples).

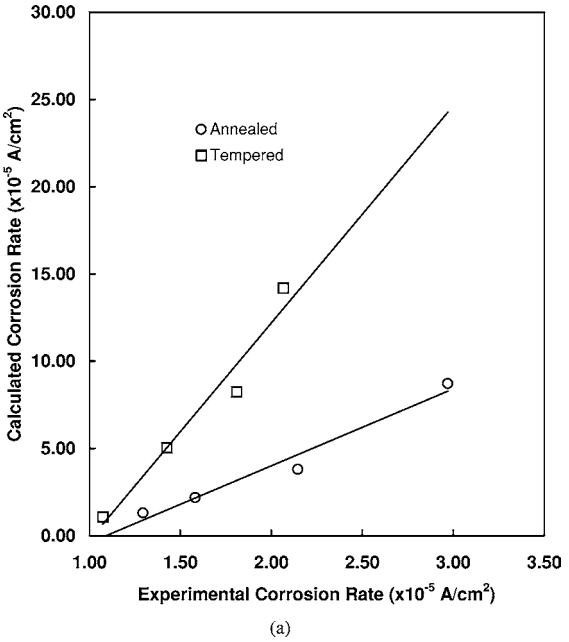

(a)

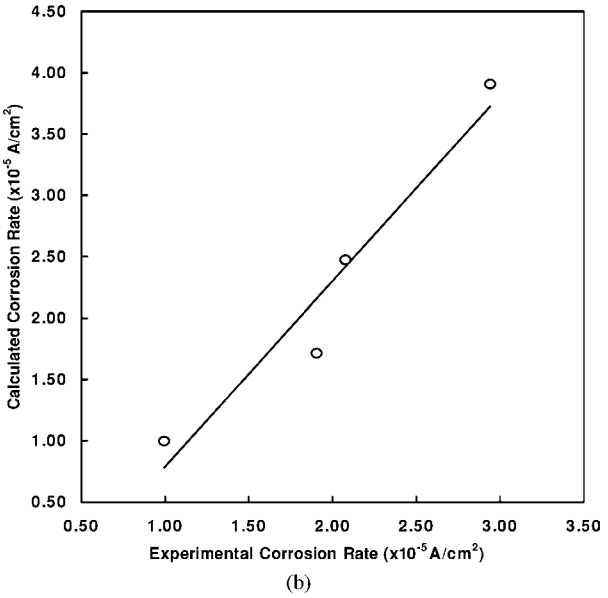

(b)

Figure 3 The relationship between the calculated corrosion rate and the experimental corrosion rate for (a) AISI 52100 steels (Annealed: $i_{corr,calculated} = 4.4115 i_{corr,experimental} - 4.8192$ with $R^2 = 0.9674$ and Tempered: $i_{corr,calculated} = 12.448 i_{corr,experimental} - 12.708$ with $R^2 = 0.9567$) and (b) AISI 1020 steels (Annealed: $i_{corr,calculated} = 1.5136 i_{corr,experimental} - 0.7259$ with $R^2 = 0.9398$).

TABLE IIB Calculated corrosion rates of eroded AISI 1020 steel

AISI 1020 steels	Corrosion rate i_a^s	Corrosion rate ($\times 10^{-5}$ A/cm^2) Amount of erodent (erosion angle 45°) No erosion	10 g	50 g	100 g
As-received	Experimental corrosion rate	1.29	1.59	2.22	2.33
	Calculated corrosion rate	1.32	4.40	9.64	17.55
Annealed	Experimental corrosion rate	1.00	1.91	2.08	2.94
	Calculated corrosion rate	1.00	1.71	2.47	3.91
Quenched	Experimental corrosion rate	1.28	1.83	2.70	2.91
	Calculated corrosion rate	1.34	7.49	8.81	16.37

4. Conclusions

The mechano-electrochemical effect has been quantitatively described in terms of the corrosion rate as a function of the change in corrosion potential and the increased strain energy, rather than in a graph or literal description of electrochemical parameters as a function of load or strain.

A mathematical relationship has been developed to describe the mechano-electrochemical effect, in which the corrosion rate is exponentially related to potential, strain energy and polarization behavior, namely:

$$i_A^s = i_A e^{\Delta E_k^s / b_a} e^{A/RT}$$

i.e., the corrosion rate (i_A^s) of an eroded specimen is ($e^{\Delta E_k^s/b_a} e^{A/RT}$) times larger than that of un-eroded specimen (i_A). This is confirmed by the experimentally measured corrosion rates, which increase with increasing erosion.

The calculated corrosion rates of annealed and tempered samples agree reasonably well with the experimentally measured corrosion rates. This shows that the mechano-electrochemical equation is valid for the electrodes where the plastic strain (microstrains) arises from the erosion process and not from prior (to erosion) heat-treatment or mechanical deformation.

References

1. D. WANG and S. ZHU, *Chinese J. Chem. Eng.* **5** (1997) 226.
2. A. ELIEZER, E. ABRAMOV and E. M. GUTMAN, *J. Mater. Sci. Lett.* **17** (1998) 801.
3. E. M. GUTMAN, G. SOLOVIOFF and D. ELIEZER, *Corr. Sci.* **38** (1996) 1141.
4. X. X. JIANG, S. Z. LI, D. D. TAO and J. X. YANG, *Corrosion* **49** (1993) 836.
5. H. SKRZYPEK and S. A. BRADFORD, *ibid.* **46** (1990) 929.
6. X. C. LU, K. SHI, S. Z. LI and X. X. JIANG, *Wear* **225–229** (1999) 537.
7. I. M. DMYTRAKH, R. AKID and K. J. MILLER, *British Corr. J.* **32** (1997) 138.
8. E. A. TRILLO, R. BELTRAN, J. G. MALDONADA, R. J. ROMERO, L. E. MURR, W. W. FISHER and A. H. ADVANI, *Mater. Character.* **35** (1995) 99.
9. Y. F. LI, G. C. FARRINGTON and C. LAIRD, *Acta Metall. Mater.* **41** (1993) 693.
10. R. STEFEC and F. FRANZ, *Corr. Sci.* **16** (1976) 161.
11. C. F. LO, W. E. MAYO, S. WEISSMANN and W. H. CULLEN, *Corrosion* **49** (1993) 675.
12. R. AKID and I. DMYTRAKH, *Fatigue & Fracture Engin. Mater. Struct.* **21** (1998) 903.
13. Z. SZKLARSKA-SMIALOWSKA, *Mater. Sci. Forum* **192–194** (1995) 11.
14. X. JIANG, L. SUN, S. LI and Y. XIAO, *ACTA Metall. Sinica* **5** (1992) 287.
15. S. K. VARMA and R. R. ROMERO, *Wear* **201** (1996) 121.
16. Y. S. WU, in "Corrosion Testing Methods of Metals" (Press of Metallurgical Industry, Beijing, 1992) p. 49.
17. M. P. HU, in "Electrochemistry in Corrosion" (Press of Metallurgical Industry, Beijing, 1989) p. 105.
18. Y. H. LIU, in "Experimental Electrochemistry" (Press of Beijing University of Aerospace and Aeronautics, Beijing, 1987) p. 35.
19. J. XIE, A. T. ALPAS and D. O. NORTHWOOD, *J. Mater. Engin. Perform.* **12** (2003) 77.
20. J. XIE, in "Characteristics and Mechanism of the Synergistic Effect Between Erosion and Corrosion," Ph.D thesis, University of Windsor, Ontario, Canada, 2001, p. 87.
21. F. MANSFELD, *Corrosion* **29** (1973) 397.
22. C. SURYANARAYANA and M. GRANT NORTON, in "X-ray Diffraction: A Practical Approach" (Plenum Press, New York, USA, 1998) p. 207.
23. D. LEWIS, D. O. NORTHWOOD and C. E. PEARCE, *Corr. Sci.* **9** (1969) 779.

Received 27 March
and accepted 14 August 2003